

Analysis of Reissner-Mindlin Orthotropic FGM Plates by the MLPG

J. Sladek¹, V. Sladek¹, P. Sölek², P.H. Wen³

Summary

A meshless local Petrov-Galerkin (MLPG) method is applied to solve thermal bending problems described by the Reissner-Mindlin theory. Functionally graded material properties with continuous variation in the plate thickness direction are considered too. A weak formulation for the set of governing equations in the Reissner-Mindlin theory is transformed into local integral equations on local subdomains in the mean surface of the plate with using a unit test function. The meshless approximation based on the Moving Least-Squares (MLS) method is employed for the implementation.

Introduction

Plate structures are widely used in many engineering structures such as aircraft, civil and ship engineering. Plates are often subjected to combinations of lateral pressure and thermal loading. However, many linear bending studies are focused only to a lateral pressure load with assumption of uniformly distributed temperature in the whole plate. The first thermoelastic analysis of plates including transverse shear effects was performed by [1]. Reddy and Hsu [2] presented analytical solution for simply supported rectangular cross-ply laminated plates under sinusoidal mechanical load and temperature is assumed to be varying linearly through the thickness. Nonlinear analysis of simply supported Reissner-Mindlin plates subjected to lateral pressure and thermal loading and resting on two-parameter elastic foundations is given by Shen [3]. Recently, functionally graded materials (FGMs) have been extensively used for engineering structures under a severe thermal load. Praveen and Reddy [4] analyzed the thermomechanical response of thick plates with continuous variation of properties through the plate thickness by FEM. Vel and Batra [5] obtained an exact solution for three-dimensional deformations of simply supported FGM rectangular plates subjected to mechanical and thermal loads.

Recently, the meshless local Petrov-Galerkin (MLPG) method has been also applied to Reissner-Mindlin plates under dynamic load by Sladek et al. [6]. Soric et al. [7] have performed a three-dimensional analysis of thick plates, where a plate is divided by small cylindrical subdomains for which the MLPG is applied. Homogeneous material properties of plates are considered in previous papers. Recently,

¹Institute of Construction and Architecture, Slovak Academy of Sciences, 84503 Bratislava, Slovakia

²Department of Mechanics, Slovak Technical University, Bratislava, Slovakia

³School of Engineering and Materials Sciences, Queen Mary University of London, Mile End, London E14NS, U.K.

Qian et al. [8] extended the MLPG for 3-d deformations in thermoelastic bending of FGM isotropic plates. In the present paper, the authors have developed a meshless method based on the local Petrov-Galerkin weak-form to solve thermal problems of orthotropic thick plates with material properties continuously varying through the plate thickness. The Reissner-Mindlin theory reduces the original 3-d thick plate problem to a 2-d problem. The Laplace-transform technique is applied to the set of governing differential equations for elastodynamic Reissner-Mindlin plate bending theory with Duhamel-Neumann constitutive equations. A unit test function is used in the local weak-form. Applying Gauss divergence theorem to the weak-form, the local boundary-domain integral equations are derived. The meshless approximation based on the Moving Least-Squares (MLS) method is applied.

Local integral equations for Reissner-Mindlin plate theory

Consider an elastic orthotropic plate of constant thickness h , with the mean surface occupying the domain Ω in the plane (x_1, x_2) . The plate is subjected to thermal loading with the temperature field $\theta(\mathbf{x}, x_3, t)$. The Reissner-Mindlin plate bending theory is used to describe the plate deformation. Then, one can write [9]

$$u_1(\mathbf{x}, t) = x_3 w_1(\mathbf{x}, t), \quad u_2(\mathbf{x}, t) = x_3 w_2(\mathbf{x}, t), \quad u_3(\mathbf{x}, t) = w_3(\mathbf{x}, t), \quad (1)$$

where $w_\alpha(x_1, x_2, t)$ and $w_3(x_1, x_2, t)$ represent the rotations around the in-plane axes and the out-of-plane deflection, respectively.

The linear strains are given by

$$\begin{aligned} \varepsilon_{11}(\mathbf{x}, t) &= x_3 w_{1,1}(\mathbf{x}, t), & \varepsilon_{22}(\mathbf{x}, t) &= x_3 w_{2,2}(\mathbf{x}, t), \\ \varepsilon_{12}(\mathbf{x}, t) &= x_3 (w_{1,2}(\mathbf{x}, t) + w_{2,1}(\mathbf{x}, t))/2, \\ \varepsilon_{13}(\mathbf{x}, t) &= (w_1(\mathbf{x}, t) + w_{3,1}(\mathbf{x}, t))/2, \\ \varepsilon_{23}(\mathbf{x}, t) &= (w_2(\mathbf{x}, t) + w_{3,2}(\mathbf{x}, t))/2. \end{aligned} \quad (2)$$

In the case of orthotropic materials, the relation between the stress σ_{ij} and the strain ε_{ij} when temperature changes are considered, is governed by the well known Duhamel-Neumann constitutive equations for the stress tensor

$$\sigma_{ij}(\mathbf{x}, t) = c_{ijkl} \varepsilon_{kl}(\mathbf{x}, t) - \gamma_{ij} \theta(\mathbf{x}, x_3, t), \quad (3)$$

where c_{ijkl} are the material stiffness coefficients. The stress-temperature modulus can be expressed through the stiffness coefficients and the coefficients of linear thermal expansion α_{kl}

$$\gamma_{ij} = c_{ijkl} \alpha_{kl}. \quad (4)$$

Next, we assume that the material properties are graded along the plate thickness, and we represent the profile for volume fraction variation by

$$P(x_3) = P_b + (P_t - P_b)V \text{ with } V = \left(\frac{x_3}{h} + \frac{1}{2} \right)^n, \quad (5)$$

where P denotes a generic property like modulus, P_t and P_b denote the property of the top and bottom faces of the plate, respectively, and n is a parameter that dictates the material variation profile. Poisson ratios are assumed to be uniform.

The bending moments $M_{\alpha\beta}$ and the shear forces Q_α are defined as

$$\begin{bmatrix} M_{11} \\ M_{22} \\ M_{12} \end{bmatrix} = \int_{-h/2}^{h/2} \begin{bmatrix} \sigma_{11} \\ \sigma_{22} \\ \sigma_{12} \end{bmatrix} x_3 dx_3 \text{ and } \begin{bmatrix} Q_1 \\ Q_2 \end{bmatrix} = \kappa \int_{-h/2}^{h/2} \begin{bmatrix} \sigma_{13} \\ \sigma_{23} \end{bmatrix} dx_3, \quad (6)$$

where $\kappa = 5/6$ in the Reissner plate theory.

The bending moments $M_{\alpha\beta}$ and shear forces Q_α for $\alpha, \beta=1,2$, can be expressed in terms of rotations, lateral displacements of the orthotropic plate and temperature

$$\begin{aligned} M_{\alpha\beta} &= D_{\alpha\beta} (w_{\alpha,\beta} + w_{\beta,\alpha}) + C_{\alpha\beta} w_{\gamma,\gamma} - H_{\alpha\beta}, \\ Q_\alpha &= C_\alpha (w_\alpha + w_{3,\alpha}), \end{aligned} \quad (7)$$

where

$$H_{\alpha\beta} = \int_{-h/2}^{h/2} x_3 \gamma_{\alpha\beta} \theta(\mathbf{x}, x_3, t) dx_3.$$

The material parameters $D_{\alpha\beta}$ and $C_{\alpha\beta}$ are given as

$$\begin{aligned} D_{11} &= \frac{D_1}{2} (1 - \nu_{21}), & D_{22} &= \frac{D_2}{2} (1 - \nu_{12}), & D_{12} &= D_{21} = \frac{\bar{G}_{12} h^3}{12}, \\ C_{11} &= D_1 \nu_{21}, & C_{22} &= D_2 \nu_{12}, & C_{12} &= C_{21} = 0, \\ D_\alpha &= \frac{\bar{E}_\alpha h^3}{12e}, & D_1 \nu_{21} &= D_2 \nu_{12}, & C_\alpha &= \kappa h \bar{G}_{\alpha 3}, \quad e = 1 - \nu_{12} \nu_{21}. \end{aligned}$$

For a general variation of material properties through the plate thickness:

$$\begin{aligned} D_{11} &= \int_{-h/2}^{h/2} x_3^2 E_1(x_3) \frac{1 - \nu_{21}}{e} dx_3, & D_{22} &= \int_{-h/2}^{h/2} x_3^2 E_2(x_3) \frac{1 - \nu_{12}}{e} dx_3, \\ D_{12} &= \int_{-h/2}^{h/2} x_3^2 G_{12}(x_3) dx_3, & C_{11} &= \int_{-h/2}^{h/2} x_3^2 E_1(x_3) \frac{\nu_{21}}{e} dx_3, \\ C_{22} &= \int_{-h/2}^{h/2} x_3^2 E_2(x_3) \frac{\nu_{12}}{e} dx_3, & C_\alpha &= \kappa \int_{-h/2}^{h/2} G_{\alpha 3}(x_3) dx_3. \end{aligned} \quad (8)$$

Equations of motion in Reissner's linear theory of thick plates the may be written as

$$\begin{aligned} M_{\alpha\beta,\beta}(\mathbf{x}, t) - Q_\alpha(\mathbf{x}, t) &= \frac{\rho h^3}{12} \ddot{w}_\alpha(\mathbf{x}, t), \\ Q_{\alpha,\alpha}(\mathbf{x}, t) + q_3(\mathbf{x}, t) &= \rho h \ddot{w}_3(\mathbf{x}, t), \quad \mathbf{x} \in \Omega, \end{aligned} \quad (9)$$

where ρ is the mass density, and throughout the paper Greek indices vary from 1 to 2. The dots over a quantity indicate differentiations with respect to time t .

To eliminate the time variable t in the governing equations (10), the Laplace-transform is applied. Then, one obtains

$$\bar{M}_{\alpha\beta,\beta}(\mathbf{x},s) - \bar{Q}_{\alpha}(\mathbf{x},s) = \frac{\rho h^3}{12} s^2 \bar{w}_{\alpha}(\mathbf{x},s) - \bar{R}_{\alpha}(\mathbf{x},s), \quad (10)$$

$$\bar{Q}_{\alpha,\alpha}(\mathbf{x},s) = \rho h s^2 \bar{w}_3(\mathbf{x},s) - \bar{R}_3(\mathbf{x},s), \quad (11)$$

where s is the Laplace-transform parameter, while \bar{R}_{α} and \bar{R}_3 are given by

$$\bar{R}_{\alpha}(\mathbf{x},s) = \frac{\rho h^3}{12} [s w_{\alpha}(\mathbf{x}) + \dot{w}_{\alpha}(\mathbf{x})], \quad \bar{R}_3(\mathbf{x},s) = \bar{q}_3(\mathbf{x},s) + \rho h s w_3(\mathbf{x}) + \rho h \dot{w}_3(\mathbf{x}).$$

The MLPG method constructs weak-forms of the above governing equations over the local arbitrary sub-domains such as Ω_s , which is a small region taken for each node inside the global domain [6]. In the Laplace-transformed domain, these equations can be converted to the following local boundary-domain integral equations

$$\int_{\partial\Omega_s^i} \bar{M}_{\alpha}(\mathbf{x},s) d\Gamma - \int_{\Omega_s^i} \bar{Q}_{\alpha}(\mathbf{x},s) d\Omega - \int_{\Omega_s^i} \frac{\rho h^3}{12} s^2 \bar{w}_{\alpha}(\mathbf{x},s) d\Omega + \int_{\Omega_s^i} \bar{R}_{\alpha}(\mathbf{x},s) d\Omega = 0, \quad (12)$$

$$\int_{\partial\Omega_s^i} \bar{Q}_{\alpha}(\mathbf{x},s) n_{\alpha}(\mathbf{x}) d\Gamma - \int_{\Omega_s^i} \rho h s^2 \bar{w}_3(\mathbf{x},s) d\Omega + \int_{\Omega_s^i} \bar{R}_3(\mathbf{x},s) d\Omega = 0. \quad (13)$$

The trial functions are approximated by the Moving Least-Squares (MLS) method [6]. Substituting the MLS-approximations into the local boundary-domain integral equations the system of linear algebraic equations of the unknown nodal values is obtained.

Numerical results

Consider a simply supported square plate with a side-length $a = 0.254\text{m}$ and the plate thicknesses $h/a = 0.05$. On the top surface of the plate a uniformly distributed temperature $\theta = 1 \text{ deg}$ is considered. The bottom surface is kept at vanishing temperature. The orthotropic mechanical properties of the plate are considered with Young's moduli $E_2 = 0.6895 \cdot 10^{10} \text{N/m}^2$, $E_1 = 2E_2$, Poisson's ratios $\nu_{21} = 0.15$, $\nu_{12} = 0.3$. The used shear moduli correspond to Young's modulus E_2 , $G_{12} = G_{13} = G_{23} = E_2/2(1 + \nu_{12})$.

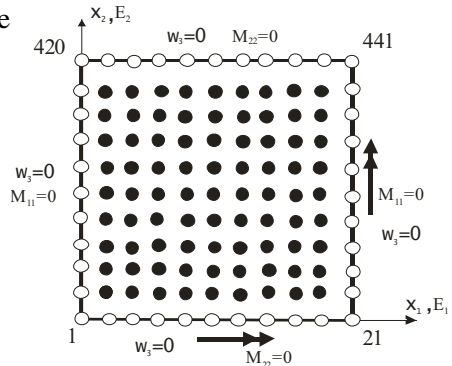


Figure 1: A simply supported square plate

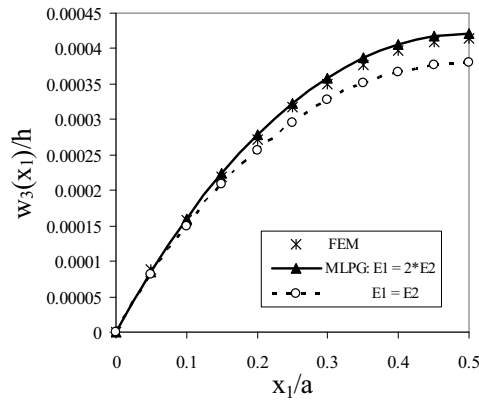


Figure 2: Influence of orthotropic material properties on the plate deflection

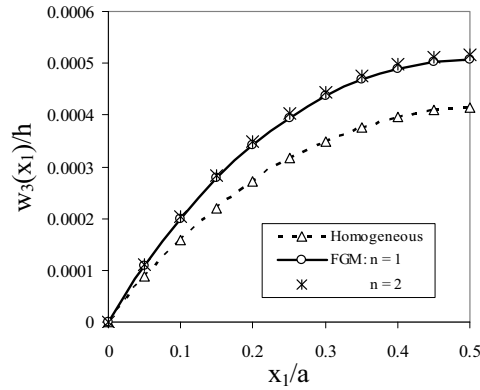


Figure 3: Variation of the deflection with the x_1 -coordinate for an isotropic square plate with FGM properties

The thermal expansion coefficients $\alpha_{11} = \alpha_{22} = 1 \cdot 10^{-5} \text{ deg}^{-1}$.

The variation of the deflection with the x_1 -coordinate at $x_2 = a/2$ of the plate is presented in Fig. 2 with assuming isotropic thermal expansion coefficients. Opposite to mechanical load case [6] the deflection is not reduced in the orthotropic plate as compared with the isotropic plate. It is due to increasing equivalent load for orthotropic plate at the same temperature distributions in both cases.

Next, functionally graded material properties through the plate thickness are considered.

The following isotropic material parameters on top side of the plate are used in numerical analysis: Young’s moduli $E_{2t} = 0.6895 \cdot 10^{10} \text{ N/m}^2$, Poisson’s ratio $\nu_{12} = 0.3$. Linear and quadratic variations of volume fraction V defined in equation (5) are considered here, and Young’s moduli on the bottom side are: $E_{1b} = E_{2b} = E_{1t}/2$. The variation of deflections with the x_1 -coordinate is given in Fig. 3.

Since Young’s modulus on bottom side is considered to be smaller than on the top one, deflection for FGM plate is larger than for homogenous plate. In both linear and quadratic variations of Young’s moduli the same surface values are considered. One can observe in Fig. 3 that the profile of the variation of material properties has negligible influence on the deflection. But the deflection is influenced by the surface values of material parameters on the bottom and top sides of the plate.

References

1. Das, M.C.; Rath, B.K. (1972): Thermal bending of moderately thick rectangular plates. *AIAA Journal*, 10: 1349-1351.

2. Reddy, J.N.; Hsu, Y.S. (1980): Effects of shear deformation and anisotropy on the thermal bending of layered composite plates. *Journal of Thermal Stresses*, 3: 475-493.
3. Shen, H.S. (2000): Nonlinear analysis of simply supported Reissner-Mindlin plates subjected to lateral pressure and thermal loading and resting on two-parameter elastic foundations. *Engineering Structures*, 23: 1481-1493.
4. Praveen, G.N.; Reddy, J.N. (1998): Nonlinear transient thermoelastic analysis of functionally graded ceramic-metal plates. *Int. J. Solids and Structures*, 35: 4457-4476.
5. Vel, S.S.; Batra, R.C. (2002): Exact solution for thermoelastic deformations of functionally graded thick rectangular plates. *AIAA Journal*, 40: 1421-1433.
6. Sladek, J.; Sladek, V.; Krivacek, J.; Wen, P.; Zhang, Ch. (2007): Meshless Local Petrov-Galerkin (MLPG) method for Reissner-Mindlin plates under dynamic load. *Computer Meth. Appl. Mech. Engn.*, 196: 2681-2691.
7. Soric, J.; Li, Q.; Atluri, S.N. (2004): Meshless local Petrov-Galerkin (MLPG) formulation for analysis of thick plates. *CMES: Computer Modeling in Engineering & Sciences*, 6: 349-357.
8. Qian, L.F.; Batra, R.C. (2004): Transient thermoelastic deformations of thick functionally graded plate. *Jour. Thermal Stresses*, 27: 705-740.
9. Reddy J.N. (1997): *Mechanics of Laminated Composite Plates: Theory and Analysis*. CRC Press, Boca Raton.